

RSC Advances



This is an *Accepted Manuscript*, which has been through the Royal Society of Chemistry peer review process and has been accepted for publication.

Accepted Manuscripts are published online shortly after acceptance, before technical editing, formatting and proof reading. Using this free service, authors can make their results available to the community, in citable form, before we publish the edited article. This *Accepted Manuscript* will be replaced by the edited, formatted and paginated article as soon as this is available.

You can find more information about *Accepted Manuscripts* in the [Information for Authors](#).

Please note that technical editing may introduce minor changes to the text and/or graphics, which may alter content. The journal's standard [Terms & Conditions](#) and the [Ethical guidelines](#) still apply. In no event shall the Royal Society of Chemistry be held responsible for any errors or omissions in this *Accepted Manuscript* or any consequences arising from the use of any information it contains.

COMMUNICATION

Bottom-up Approach to Engineer a Molybdenum-doped Covalent-Organic Framework Catalyst for Selective Oxidation Reaction

Cite this: DOI: 10.1039/x0xx00000x

Received 00th January 2012,
Accepted 00th January 2012

DOI: 10.1039/x0xx00000x

www.rsc.org/

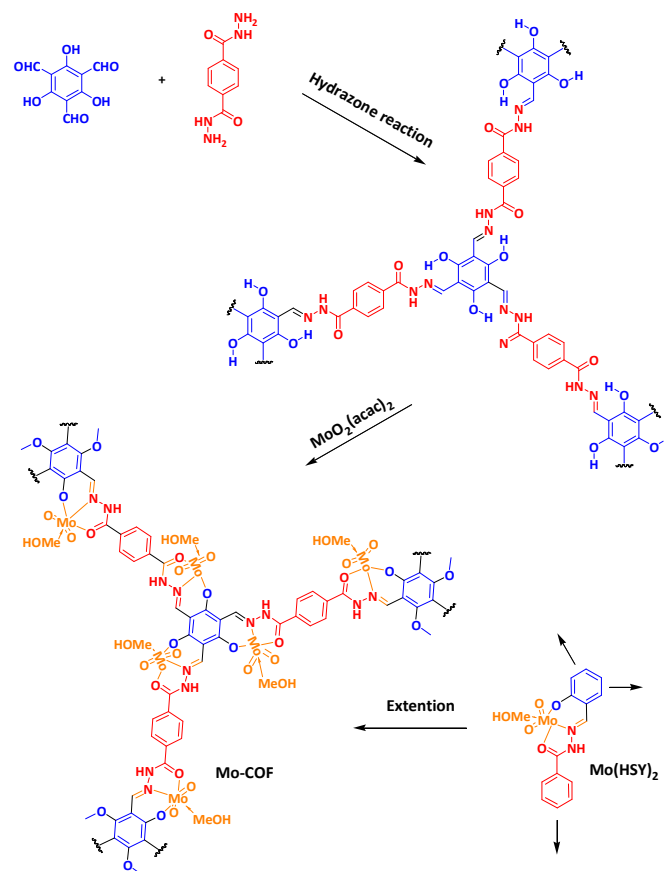
Weijie Zhang,^a Pingping Jiang,^{a*} Ying Wang,^a Jian Zhang,^b Yongxue Gao,^a and Pingbo Zhang^a

We have realized a readily accessible molybdenum-doped covalent-organic framework catalyst (Mo-COF) linked by hydrazone linkage *via* a facile two-step bottom-up approach. Here, the reported Mo-COF catalyst as an open nanochannel-reactor presents promising catalytic property for selective oxidation reaction.

Selective oxidation is a field of increasing interest in relation to the design of highly active catalysts. Among various catalysts, molybdenum has received huge attention, due to possessing a large number of stable and variable oxidation states.¹ Additionally, the coordination numbers can vary from four to eight as well as its relevance to the active sites of majority of molybdo-enzymes. As a consequence, it is of further importance to develop molybdenum catalysts acting as an effective peroxidase mimic. However, the application of molybdenum complexes as homogenous catalyst in solution is usually challenging because of the formation of catalytically inactive dimers during the process.² Although combining homogenous catalyst with insoluble materials has been considered as a promising strategy, this method inevitably dilutes the density of active centres (0.2-0.4 mmol/g).³ Therefore, there is an urgent need to circumvent these challenges by developing novel Mo-based catalysts with high active site density.

Recent years, the inclusion of catalytic functionality into covalent organic frameworks (COFs) is one of the flourishing fields of research.⁴ COF is a novel class of porous crystalline organic materials assembled from molecular building blocks by linking light elements (e.g. B, C, N, O) *via* covalent bond formation (boronic acid trimerization, boronate ester formation, the Schiff base reaction, hydrazone and squaraine linkage) in a periodic manner.⁵ Apart from that, ordered one-dimensional open channels represent the typical porous structure of two-dimensional COFs, which provides a desirable micro-environment for incorporation of open docking sites into ordered alignment. Meanwhile, the crystallinity of COFs enables direct visualization of structure and makes it possible to get a detailed insight into the relationship between the structure and the catalytic activity by structural interrogation. Nonetheless, it is still limited so far to develop efficient COF catalysts.

Here, we reported a facile bottom-up strategy to direct a molybdenum-doped covalent organic framework, henceforth denoted as Mo-COF, acting as an efficient catalyst in selective oxidation. To be more precise, the Mo sites were ordered into the channel walls of π -arrays through a robust coordination between



Scheme 1 Formation of molecular building blocks of Mo-COF.

molybdenyl acetylacetonate ($\text{MoO}_2(\text{acac})_2$) and π -connected benzoyl salicylal hydrazone ligand, forming an effective nanochannel-reactor. This design allows an easy access of guest molecules through the 1D channel to the docking sites (Scheme 1). Based on the structural feature, the vertex unit of this COF plays two different roles in this bottom-up strategy, that is, connecting the building blocks and providing free positions for loading Mo sites. Thus, this total strategy can be divided into two steps: In the first step, a reaction leads to the formation of a crystalline hydrazone-linked COF with a predetermined topological design using appropriate symmetry combinations ($C_2 + C_3$) of building blocks framework,^{5b, 5c} and the second step is to introduce Mo resource into this porous network. Overall, the aforementioned points provide a fundamental understanding of this heterogeneous catalyst about its accessibility of the open channels. To the best of our knowledge, there appears to be no report on COF catalyst synthesized using this approach.

The valence state of the Mo element in Mo-COF catalyst was characterized by XPS technology. The survey scan of the Mo 3d region was shown in Figure S3. It showed Mo 3d lines at 232.6 eV ($3d_{5/2}$) and 235.6 eV ($3d_{3/2}$), which was the characteristic of molybdenum metal in +6 oxidation state.⁶ On the other hand, the Mo of $3d_{5/2}$ for Mo-COF shifted positively by in comparison with that of $3d_{5/2}$ for standard $\text{MoO}_2(\text{acac})_2$ (233.3 eV).⁷ This positive shift indicated the strong coordination of Mo with the benzoyl salicylal hydrazone groups of COF; this group further withdrew electrons from Mo which made the Mo species more electron-deficient. Moreover, Figure S4 showed the UV-vis was electronic absorption spectra of the complex Mo-benzoyl salicylal hydrazine Schiff base, namely $\text{Mo}(\text{HSY})_2$. The absorption band for ligand-metal ($\pi^* \rightarrow d\pi$) charge transfer transition centred at 400 nm.^{3a} Then, the steady-state electronic absorption spectra (Steady-state UV-vis) were informative for detecting the formation of charge transfer in insoluble Mo-COF material. As COF for example, there was a wide absorption band around 400-500 nm, which indicated the extended π conjugation over the 2D sheet of the COF.^{4b} It is, however, notable that the higher energy ligand transition of Mo-COF was moved to lower energy relative to $\text{Mo}(\text{HSY})_2$ and COF. This suggests that there was a significant effect on the electronic energy levels of Mo sites.

Our reported Mo-COF was obtained as orange-red microcrystalline powder that remained insoluble in common organic solvents (See the Supporting Information). As shown in Figure S5, powder X-ray diffraction (PXRD) patterns of COF showed the most intense peaks at 3.2° , which corresponded to d_{100} plane reflections. XRD studies on COF and Mo-COF in Figure S5 indicated certain accordance between experimental patterns and the simulated patterns based on the modelled structure. Although the intensity of XRD pattern for COF and Mo-COF was poor, the experimental XRD pattern of COF and Mo-COF also partly matched well with the simulated pattern of the AA stacking model, relative to AB stacking model (Figure S6). The cross-linking of COF network may give rise to uncertain conformation (20° - 30°). Hence, we proposed a structure close to the $P6/m$ space group for COF. The unit cell values of COF were calculated to be $a = b = 31 \text{ \AA}$ and $c = 3.4 \text{ \AA}$ by Material Studio software. In addition, the intensity of d_{100} reflection of Mo-COF decreased and d_{100} spacing shifted to a higher angle compared with pristine COF. This suggested a decrease in uniformity of its porous structure and hole size due to the catalytic sites being encapsulated into the channels. On the other hand,

there was no obvious framework collapse and any crystalline phase of $\text{MoO}_2(\text{acac})_2$ species was also not observed (Figure S5).

The new peak at 911 cm^{-1} confirmed the existence of the Mo-O bond in Mo-COF, relative to pure COF (Figure S7). Interestingly, the Mo-O peak at 905 cm^{-1} in $\text{MoO}_2(\text{acac})_2$ shifted to a higher peak at 911 cm^{-1} (Figure S8). This result proved the successful incorporation into the framework backbone through stable coordination bond. In addition, compound COF and Mo-COF both exhibited a typical type III isotherm with a surface area of $244 \text{ m}^2/\text{g}$ for CPF-1 and $63 \text{ m}^2/\text{g}$, respectively (Figure S9). The prepared COF showed N_2 adsorption isotherms with low BET surface areas. It can be speculated that the synthesized COF adopt a thin layer morphology. Due to the thin-layered structures, long-rang pore formation was hindered, rendering N_2 adsorption possible only in the shallowest, most accessible pores.⁸ Thermogravimetric analysis (TGA) of the activated COF had no obvious weight loss until 280°C (Figure S10), leading to complete collapse of COF framework. One may notice that the frameworks of Mo-COF started to decompose around 260°C , which might be attributed to destruction of hydrogen bonding located in this 2D framework.⁹ SEM revealed that Mo-COF was composed of uniform micrometre-scale bet morphology of dimension ca. 200 nm (Figure S11).

The inductively coupled plasma atomic mass spectrometry analysis (ICP-MS) results showed that the density of active Mo sites reached as high as 2.0 mmol/g , which was also in good agreement with the data obtained from the TG studies. The highest amount of theoretical Mo sites in Mo-COF is 3.6 mmol/g . The Mo content of Mo-COF was found to be 5-10 times higher than ever reported amount of Mo complex grafted on insoluble materials, like mesoporous sieve, MWCNT and polymer.^{3a, 10} In this regard, the bottom-up strategy could facilitate catalyst with a high active sited density, owing to their accessibility, facile derivatization and ability to bind a wide variety of metal ions, like Cu, Mn and W ions.

Table 1. Scope of Mo-COF catalysed epoxidation of cyclohexene^[a]

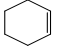
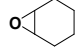


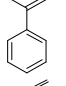
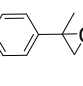
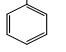
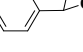
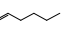
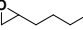
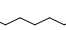
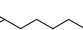
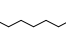
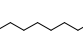
Entry	Catalyst	Conversion (%) ^[b]	Selectivity (%) ^[c]
1	Mo-COF	>99	71
2	$\text{Mo}(\text{HSY})_2$	29	68
3	blank	19	5
4	Filtrate ^[d]	20	4
5	Mo-COF ^[e]	96	70
6	COF	32	7

[a] substrate (1.0 mmol), TBHP (2.0 mmol), catalyst (0.01 mmol), 1,2-dichloroethane (2.0 mL) and bromobenzene (50 mg) as internal standard sealed in a Teflon-lined screwcap vial were stirred at 80°C for 6h. [b] Conversion [%] and [c] selectivity [%] were determined by GC using an SE-54 column. [d] After catalytic assay for Mo-COF. [e] After fourth cycles.

To show that Mo-COF was catalytically active, we evaluated the performance of Mo-COF as a nanochannel-reactor in the context of epoxidation of cyclohexene. Catalytic assays for the epoxidation of cyclohexene were carried out using *tert*-butyl hydroperoxide (TBHP) as oxidant in 1,2-dichloroethane. Control experiments were conducted for Mo-COF, homogeneous $\text{Mo}(\text{HSY})_2$

and a blank under the same conditions. As revealed in Table 1, Mo-COF showed efficient catalytic activity of epoxidation of cyclohexene in terms of both conversion (99 % over 6 h) and selectivity (71 % epoxide product) compared to Mo(HSY)₂ (29 % conversion and 68 % epoxidized selectivity, entry 2), which was basically as inactive as the blank (19 % conversion, 5 % selectivity). The low activity observed for homogeneous Mo(HSY)₂ could be attributed to catalyst deactivation as a result of the oxo-bridged dimer formation.² Therefore, the Mo-COF outperformed the 2D layered in epoxidation of cyclohexene, thus highlighting the high efficiency of 2D network-based nanochannel-reactor in Mo-COF by its structural resistance to formation of catalytically inactive species. The supernatant from oxidation of cyclohexene after filtration through a regular filter did not afford any additional oxidation product, thus strongly confirming the heterogeneous nature of the Mo-COF catalyst (Table 1, entry 4 and Figure S12). Mo-COF could be reused for four cycles without significant drop in its catalytic activity (Table 1, entry 5).

Table 2. Scope of Mo-COF catalysed epoxidation of alkenes.^[a]

Entry	Substrate	product	Conversion (%) ^[b]	Selectivity (%) ^[c]
1			>99	71
2			80	>99
3			71	80
4			62	86
5			42	>99
6			20	>99
7			5	>99

[a] Olefin (1.0 mmol), TBHP (2.0 mmol), catalyst (0.01 mmol), 1,2-dichloroethane (2.0 mL) and bromobenzene (50 mg) as internal standard sealed in a Teflon-lined screwcap vial were stirred at 80 °C for 6h. [b] Conversion [%] and [c] selectivity [%] were determined by GC using an SE-54 column.

The epoxidation of different olefin substrates of various molecular sizes was also investigated. Oxidation of cyclohexene gave 99 % conversion after 6 h. When cyclooctene was employed with a larger ring, the substrate consumption decreased rapidly to 80 % after 6 h (Table 2, entry 2), which was much lower than the conversion obtained by the cyclohexene as substrate. As shown in Figure S13, 96 % of cyclooctene would be converted into oxide after 24 h. We also noticed that the comparably low conversion of styrene epoxides was related with the low electron density of double bond which usually reduced their nucleophilicity toward electrophilic oxygen of catalytic intermediate.¹¹ From the structural point, iso-propenylbenzene also has a phenyl ring connecting the double bond, while an electron-donating group was located beside the double bond, which increased the electron density of double bond (Table 2, entry 3). So the conversion of iso-propenylbenzene

(conversion 71 %) was higher than that of styrene (conversion 62 %). Obviously, increasing the length of linear alkenes triggered lower epoxide yield for Mo-COF catalyst, but remained an excellent selectivity (Table 2, entry 5-7). Taken together, the above results indicated that the COF catalyst exhibited reagent size selectivity and the oxidation reaction was indeed occurring inside the nanochannel of framework.

Upon completion of the reaction, the catalyst could be easily recovered in nearly quantitative yield by simple filtration and can be used repeatedly without significant degrading the catalytic performance after four cycles (Figure S14). The FT-IR measurement (Figure S15) also showed that the recovered Mo complex retained. More importantly, ICP-MS analysis of the product solution indicated little loss of the metal ions about 0.01 % of from the structure per cycle.

Conclusions

In summary, an efficient π -connected organomolybdenum catalyst with a high active site density (2.0 mmol/g) was successfully constructed *via* the bottom-up strategy. This novel nanochannel-reactor inherited a typical porous structure of two-dimensional COF, providing a desirable micro-environment for selective oxidation. Furthermore, the catalytic details evidenced that Mo-COF displayed an excellent performance on catalysing selective oxidation of different substrates. These results will open a way to design COF based catalyst and help to further understand the relationship between material structure and catalytic activity by structural interrogation.

Special thanks to Dr. Liu from East China University of Science and Technology for his help on test of XPS and Steady-state UV-vis test. This work was supported financially by the National "Twelfth Five-Year" Plan for Science & Technology (2012BAD32B03), the National Natural Science Foundation of China (20903048) and the Innovation Foundation in Jiangsu Province of China (BY2013015-10).

Notes and references

^a The Key Laboratory of Food Colloids and Biotechnology, School of Chemical and Material Engineering, Jiangnan University, Wuxi 214122, P.R. China. E-mail: ppjiang@jiangnan.edu.cn

^b School of Chemistry and Environmental Science, Lanzhou City University, Lanzhou 730000, P.R. China

Electronic Supplementary Information (ESI) available: [¹H]NMR, XPS, UV-vis, FT-IR, PXRD, Crystal Data, TG analysis and catalytic details]. See DOI: 10.1039/c000000x/

- (a) M. R. Maurya, *Curr. Org. Chem.*, 2012, **16**, 73; (b) M. J. Romo, M. Archer, I. Moura, J. J. G. Moura, J. LeGall, R. Engh, M. Schneider, P. Hof and R. Huber, *Sci.*, 1995, **270**, 1170.
- (a) A. Rezaeifard, M. Jafarpour, H. Raissi, M. Alipour and H. Stoeckli-Evans, *Z. Anorg. Allg. Chem.*, 2012, **638**, 1023; (b) J. M. Sobczak and J. J. Ziolkowski, *Appl. Catal. A: Gen.*, 2003, **248**, 261; (c) C. J. Doonan, D. A. Slizys and C. G. Young, *J. Am. Chem. Soc.*, 1999, **121**, 6430.
- (a) M. Bagherzadeh, M. Zare, T. Salemnoush, S. Özkur and S. Akbayrak, *Appl. Catal. A: Gen.*, 2014, **475**, 55; (b) H. Chen and A. A. Adesina, *Appl. Catal. A: Gen.*, 1994, **112**, 87; (c) A. Castro, J. C. Alonso, P. Neves, A. A. Valente and P. Ferreira, *Eur. J. Inorg. Chem.*, 2010, **2010**, 602.
- (a) L. Li, Z. Chen, H. Zhong and R. Wang, *Chem. Eur. J.*, 2014, **20**, 3050; (b) X. Chen, N. Huang, J. Gao, H. Xu, F. Xu and D. Jiang, *Chem. Commun.*, 2014, **50**, 6161; (c) S. Y. Ding, J. Gao, Q. Wang, Y. Zhang, W. G. Song, C. Y. Su and W. Wang, *J. Am. Chem. Soc.*, 2011, **133**, 19816; (d) V. S. P. K. Neti, X. F. Wu, S. G. Deng and L. Echegoyen, *Poly. Chem.*, 2013, **4**, 4566.
- (a) J. A. P. Cote, A. I. Benin, N. W. Ockwig, M. O'Keefe, A. J. Matzger and O. M. Yaghi, *Sci.*, 2005, **310**, 1166; (b) S. Y. Ding and W. Wang, *Chem. Soc. Rev.*, 2013, **42**, 548; (c) X. Feng, X. Ding and D. Jiang, *Chem. Soc. Rev.*, 2012, **41**, 6010.

6. Z. Zhang, B. Liu, K. Lv, J. Sun and K. Deng, *Green Chem.*, 2014, **16**, 2762.
7. S. J. N. Burgmayer, H. L. Kaufmann, G. Fortunato, P. Hug and B. Fischer, *Inorg. Chem.*, 1999, **38**, 2607.
8. B. P. Biswal, S. Chandra, S. Kandambeth, B. Lukose, T. Heine and R. Banerjee, *J. Am. Chem. Soc.*, 2013, **135**, 5328.
9. S. Kandambeth, A. Mallick, B. Lukose, M. V. Mane, T. Heine and R. Banerjee, *J. Am. Chem. Soc.*, 2012, **134**, 19524.
10. (a)E. Zamanifar, F. Farzaneh, J. Simpson and M. Maghami, *Inorganica Chimica Acta*, 2014, **414**, 63; (b)B. Gao, M. Wan, J. Men and Y. Zhang, *Appl. Catal. A: Gen.*, 2012, **439-440**, 156; (c)F. Esnaashari, M. Moghadam, V. Mirkhani, S. Tangestaninejad, I. Mohammadpoor-Baltork, A. R. Khosoropour, M. Zakeri and S. Hushmandrad, *Polyhedron*, 2012, **48**, 212.
11. (a)M. H. Xie, X. L. Yang, Y. He, J. Zhang, B. Chen and C. D. Wu, *Chem. Eur. J.*, 2013, **19**, 14316; (b)W. Zhang, P. Jiang, Y. Wang, J. Zhang, J. Zheng and P. Zhang, *Chem. Eng. J.*, 2014, **257**, 28; (c)